J. Fluid Mech. (1993), *vol.* 246, *pp.* 653–674

Some experimental observations of secondary motions in a confined vortex flow

By ROBERT A. GRANGER

Professor of Mechanical Engineering, US Naval Academy, Annapolis, MD 21402-5042, USA

(Received 8 April 1991 and in revised form 25 August 1992)

Three decades have passed since vortex breakdown was first identified as a natural fluid flow phenomenon. Three key theories have been proposed to explain the phenomenon: hydrodynamic instability, conjugate states and flow stagnation. Despite a considerable amount of theoretical and experimental investigation, there is still nothing approaching a completely satisfactory theory of vortex breakdown. In addition, there is no agreement on a complete physical description of the structure of vortex breakdown. The present experimental investigation may substantiate a few earlier conjectures. We discuss an experimental finding that might help clarify the phenomenon through the use of flow visualization and laser-Doppler velocimetry. Experimental measurements substantiate earlier measurements and theoretical calculations of the velocity field. The evidence suggests that there is a connection between criticality and instability.

1. Introduction

This paper briefly presents the results of a simple experiment that was made to investigate the fundamental nature of secondary motions in a confined vortex. It is the opinion of the author that the phenomena observed have considerable implications. Examining the secondary motions suggested certain conclusions that may prove a key to understanding the nature of breakdown in confined vortex flows. It should be pointed out that the pursuit of examining the velocity field after vortex breakdown led to the accidental discovery of secondary motions. However, before discussing the description of the experiment, a brief review of the history of vortex breakdown might be helpful.

Reviews of theoretical, numerical and experimental studies in vortex breakdown and stability of vortex filaments are found in Murthy (1971), Hall (1972), Widnall (1975), Leibovich (1978) and Wedemeyer (1982). However, perhaps the most current and complete account and certainly the most lucid historical presentation of the study of vortex breakdown is that given by Escudier (1988). Escudier traces the investigative beginnings of the field in 1957 through early observations of the breakdown of leading-edge vortices from delta wings to the period when theoreticians proposed explanations of its physical behaviour. The investigations pivoted about one of three key ideas concerning the nature of vortex breakdown: instability, wave motion, and stagnation or separation. To date, there is still no general agreement as to which idea is all-encompassing or even which predicts with greatest accuracy the physical structure of the breakdown. Escudier (1988) cites over 127 of the more than 600 existing references on the subject: the number suggests the widespread interest in this classic fluid dynamics phenomenon. The range of vortex breakdown

applications is impressive. In external vortex flows, vortex breakdown is evident in the behaviour of delta swept wings causing lift, drag and pitching moment deterioration, buffeting, unsteadiness and loss of control. All shear flows past a corner result in the formation of a horseshoe vortex and its obliteration downstream from vortex breakdown (a problem which is important in antisubmarine warfare). Vortex breakdown is found in flow past the junction of two orthogonal bodies (like wing and fuselage) and in the erosion of sediment past pilings. A number of geostrophic vortices, such as tornados, have predominant breakdowns in their core.

Confined vortices also exhibit breakdown. Flame stabilization in combustion chambers, flows in the outlet casings of axial turbines and compressors and flows in vortex valves and bathtub vortices may have undesirable stability effects at a certain Reynolds number as a result of the internal geometry and flow creating the vortex breakdown.

The comprehensive problem under consideration relates to the spontaneous breakdown of a primary helical steady vortex motion and of its obliteration by motions resulting from the breakdown and spreading afield. Such breakdown is readily observed in larger vortices occurring in shear layers. As the starting point of the present study, we shall consider a familiar case: that of a confined axisymmetric vortex in an upright circular cylinder with stationary walls and having a centrally located small sink at one end of its axis.

The fluid dynamics problem can be divided into four major aspects of inquiry under the following topics:

(*a*) the structure of the steady vortex sink;
(*b*) the response near the core of the flow pattern to steady or non-steady perturbations;
(*c*) the origins and nature of secondary motions arising in the perturbed field of a vortex sink; and
(*d*) the effect of the boundary layer and of secondary motion upon the flow patterns of a vortex sink.

Let us briefly survey these four aspects as they pertain to the present investigation. Consider the structure of an undisturbed vortex. The structure of a confined steady vortex sink flow is dictated by both outer and inner boundary conditions, and thus vortex structure varies for different vortex tube configurations. For example, if one were interested in the swirling fluid motion in a straight cylindrical tube with a tangential inlet slit and an axial outlet contraction, one would reference the work of Escudier, Borstein & Zehnder (1980), Escudier & Zehnder (1982), Escudier (1988), Sarpkaya (1971), Faler & Leibovich (1977), Garg & Leibovich (1979), Chanaud (1965), Church, Snow & Agee (1977), Lugt (1962), and Cassidy & Falvey (1970), among others. In the present investigation, the vortex tube configuration consists of a stationary cylindrical surface composed of numerous equally spaced inlet slits and a *very small axial sink*. The velocity fields of the two dissimilar vortex tube configurations are similar in trends but different in values, as can be seen by comparing the results of Granger (1966, 1972) with Escudier, Borstein & Maxworthy (1982).

The response within and near the core of a confined vortex flow to steady or unsteady perturbations has been extensively studied (see the survey paper Escudier 1988). In addition, the reader should consult Murthy (1971), Hall (1972), Leibovich (1978, 1983) and Wedemeyer (1982) for descriptions of the structure of the vortex breakdown in both external and internal flows. Granger (1968, 1973) discusses some

of the properties of the breakdown, such as its velocity, for a variety of closure conditions.

The literature on the origin and nature of secondary motions arising in the perturbed field of a vortex sink is somewhat scanty. One of the earliest treatments on the subject was by Thomson (1910). This was followed by Morgan (1951) and Oser (1957). More recently, exploratory experimental investigations were presented by Weske & Rankine (1963), who examined motions in the region of the core of a vortex which exhibit peripheral vorticity. They devised a number of experiments that furnished evidence that concentrations of vorticity were periodic about the perimeter. One should also study the discussion on the stability of vortex filaments by Widnall (1975), which in part is related to the present topic. Finally, a brief discussion of some experimental results is given by Escudier *et al.* (1982), recently brought to the author's attention. One figure in the paper bears a remarkable similarity to the findings of the present paper.

The effect of the boundary layer and of secondary motion upon the flow patterns of a vortex sink was first comprehensively treated by Rott & Lewellen (1966). Their paper posed a theoretical formulation of the problem, and it discussed exact similarity solutions and the limits at which the effects of transverse pressure gradient and curvature became predominant. Rott & Lewellen used a general momentum integral solution for both laminar and turbulent flows, applying a simplified form obtained from similarity properties to include shear laws applicable in turbulent flow. Since the present investigation did not address the influence of the boundary layer, this aspect will not be discussed further.

As this brief survey suggests, the subject of vortex breakdown has resulted in considerable observational, experimental, numerical and theoretical investigations. The phenomenon concerns the tendency of a vortex possessing both axial and circumferential velocities (and small radial velocity) suddenly to jump, or make a transition, from one state to another. This transition is called *breakdown*, and it arises from a perturbation introduced along the centreline of the vortex. As pointed out earlier, a number of investigators have compared the breakdown to a number of familiar flow phenomenon: (i) axisymmetric, asymmetric, spherical or spiral disturbances; (ii) solitary or inertia waves, shock wave, hydraulic jump, or transition between two flow states; and (iii) stagnation or a pseudo-stagnation state.

A number of theoreticians suggest that hydrodynamic instability (item (i)) is the cause of vortex breakdown. Since the flow in the wake is most often unstable (for all cases except for the spherical disturbance), one cannot discuss the possibility that instability plays no role in vortex breakdown even though upstream of the breakdown the flow is stable. The question seems to revolve around whether the breakdown is a direct or indirect consequence of instability. An extensive review of papers on the role that hydrodynamic instability plays in vortex breakdown is given by Leibovich (1983).

There is another large group of investigators who believe that the breakdown is some sort of wave motion (item (ii)). Squire (1960) postulated that if standing waves existed along the vortex axis, then disturbances will move upstream along the centreline, resulting in breakdown at some critical location or critical Reynolds number. One fault with Squire's theory is that the abrupt change in the breakdown's structure cannot be predicted. Benjamin (1962) suggested that vortex breakdown is a transition between two conjugate states, a direct analogy with the hydraulic jump in open channel flow. One fault with Benjamin's theory, however, is that the subcritical conjugate has a greater momentum flux than the supercritical.

(a)

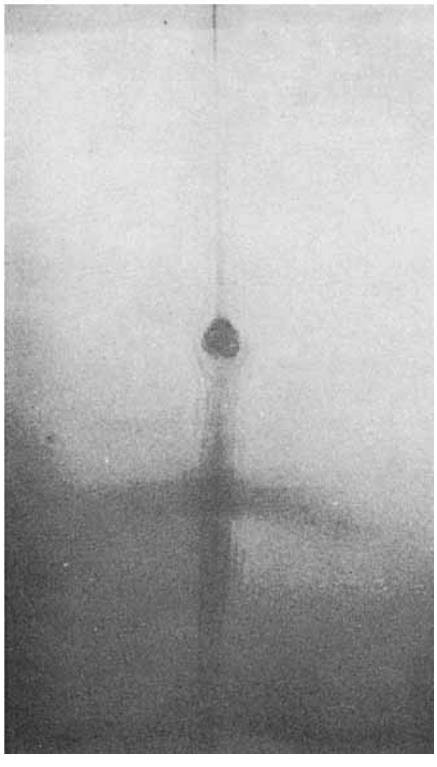

FIGURE 1 (a). For caption see facing page.

Finally, there is a group of investigators who view vortex breakdown as some feature of flow stagnation along the vortex axis (item (iii)). This view results from an examination of the quasi-cylindrical form of the Navier–Stokes equations. The calculation breaks down when the stagnation point is approached, largely due to the existence of very large axial gradients. An interesting result of this viewpoint is that one of the proponents, Bossel (1969), predicted that swirl velocities reversed their direction within the breakdown bubble. Experimental evidence in the present investigation does, indeed, reveal an annular region outside the vortex core that has reversed swirl velocities. Bossel's calculation was considered a curious anomaly and was discussed by many at the time, but it was never the subject of any sustained experimental scrutiny.

The three viewpoints (items (i)–(iii)) above are not consistent in their conclusions, and thus the controversy over which theory is correct continues to this day.

Efforts to reach a complete understanding of the structure of the flow inside the disturbance have been severely limited since any slight random movement of the position of the breakdown renders measurements made with a mechanical device meaningless. The breakdown is hypersensitive to any form of disturbance as is illustrated by the following photographs using flow visualization. Figure 1 (a) is an unusual photograph of a wave of spherical shape travelling towards the free surface. Fluid contained within the sphere appears as a ring vortex and travels with the wave. The bullet-shaped head of the disturbance, comparable to a shock wave, is followed by a laminar wake extending to its origin. If no disturbances exist in the viscous core, the spherical disturbance will remain spherical until the core radius expands to some

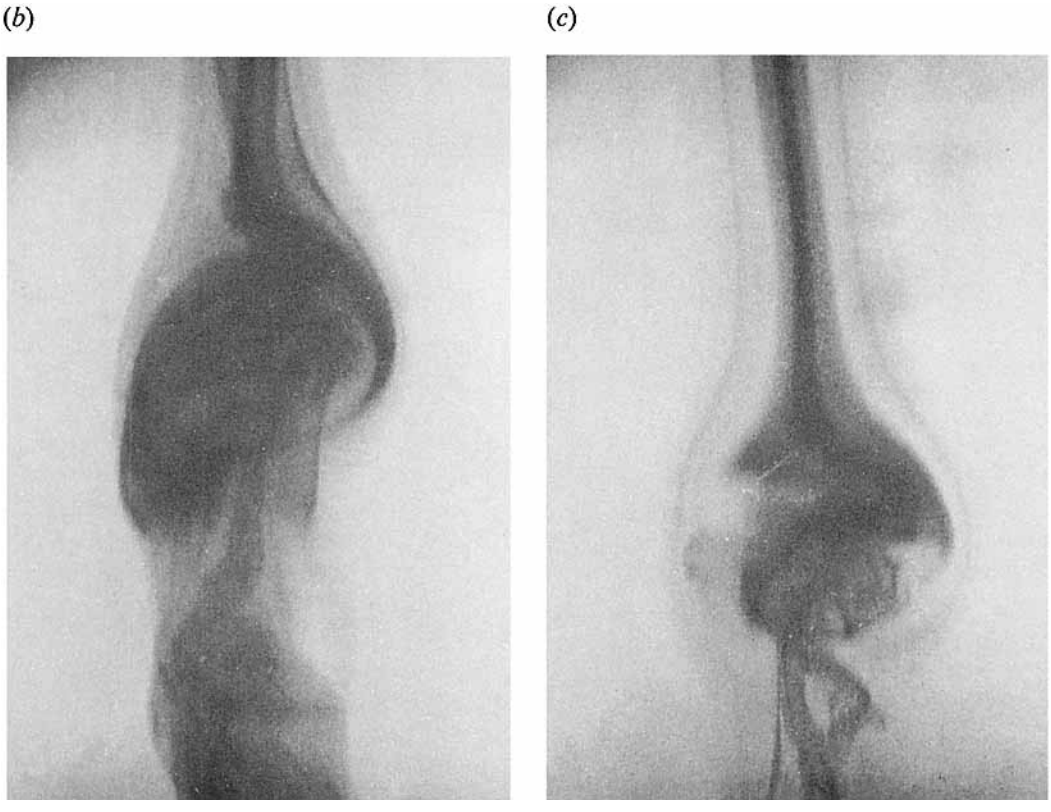

FIGURE 1. (*a*) Spherical wave propagating along the vortex centreline. Note the laminar wake. $\Gamma_\infty = 20$ cm^2/s, $\xi = 0.73$. (*b*, *c*) Vortex breakdown: (*b*) First stage, $\Gamma_\infty = 22$ cm^2/s, $\xi = 0.77$; (*c*) second stage, $\Gamma_\infty = 22$ cm^2/s, $\xi = 0.48$. Shutter speed $= 4 \times 10^{-3}$ s, $r_0 = 0.635$ cm.

critical radius. This observation lends support to the opinion that vortex breakdown is an instability phenomenon since without disturbances the spherical wave will not break down. However, if disturbances do exist in the core, the spherical wave quickly deforms, the vortex ring inside the wave distorts and the wave eventually transforms into two vortex filaments as shown in figure 1(*b*). The vortex breakdown is very similar in shape to the classic Lambourne & Bryer (1962) vortex breakdown over a delta wing at high angle of attack. In time, the disturbance decays into the spiral vortex of figure 1(*c*).

Having the capability to produce a variety of different vortex breakdown configurations, the author performed an experimental investigation to help shed light on which of the three key explanations, if any, is the correct explanation for vortex breakdown. In particular, if disturbances die out in the viscous core (which they do), where are there disturbances that can precipitate vortex breakdown?

2. The apparatus

The experimental apparatus was a duplicate of that described by Granger (1972) so that data obtained from laser Doppler velocimeter (LDV) measurements could be compared against theory and previous measured results presented in the above reference.

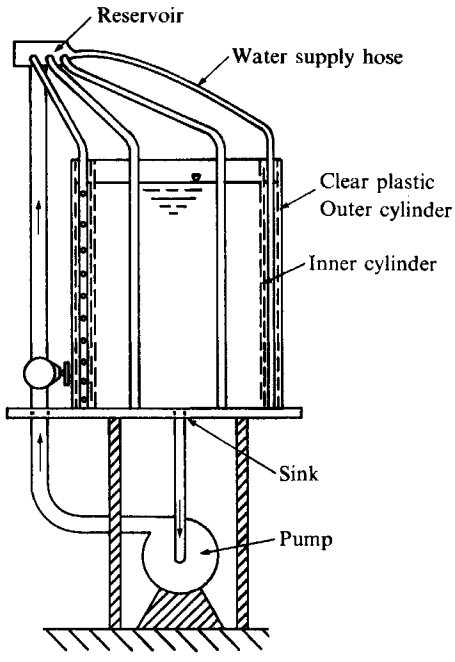

FIGURE 2. Schematic of the vortex generator. A 16.6 cm wide flat acrylic strap 1.22 cm long is attached to the outer cylinder to provide a window for the laser beam.

The experimental measurements were conducted in an upright tank 1.22 m high and 0.58 m in diameter that was constructed of two concentric cylinders made of acrylic sheets. The outer acrylic cylinder was firmly mounted on a horizontal tank table to create a watertight container. A 1.22 m long by 0.166 m wide flat acrylic window was formed along the outer cylinder to prevent the cylinder from acting as a lens for the laser beams. The inner plastic cylinder was inserted into the outer cylinder to form a narrow annular space of 12.7 mm radial width. It was fixed so as not to rotate. The other end of the tank was open to the atmosphere. The tank could be filled with water from an external source to whatever depth was desired. As shown in figure 2, the water was circulated by a centrifugal pump placed in the external closed circuit. The pump withdrew water through a centred circular plug located in the tank table. Three different plugs of diameters 6.35, 12.7 and 19.05 mm could be used. Thence the water passed through a flow-rate meter, past a remote-control shutoff valve, through a globe valve to a header and into eight vertical feeder tubes. Each feeder tube was placed equal distances apart in the annular region created by the two cylinders. Each feeder tube was 12.7 mm in diameter and was perforated with equally spaced holes 1.59 mm in diameter and 50.8 mm apart along its axial length. The bottom end of each tube was sealed and the top end was connected to the header by a flexible tube. The water in the annular region was distributed to the body of water filling the central space of the tank through numerous rectangular orifices uniformly spaced in the inner cylinder wall. Each orifice was provided with a hood to direct the jets of water so they would leave the annular region nearly tangentially along the inner cylindrical surface into the central region of the vortex. In this manner, circulation was imparted to the body of water with little to no disturbance.

The circulated water could be continuously withdrawn at the sink and injected

along the outer boundary of the main body of circulating water while the height of the water level remained constant.

The flow in the inner cylinder was steady and laminar for all tests with the shutoff valve remaining open. With the exception of an inner cylindrical region of radius approximately 2.5–5 cm, the ambient circulation Γ_∞ could be varied from one experiment to the next by changing the rate of flow through the sink. At circulations lower than 18 cm^2/s, precessional oscillations of large period make systematic measurements difficult; at circulations larger than 190 cm^2/s, entry of air alters the flow in the region of the core and thereby precludes its investigation. Hence, the range of ambient circulations used was $18 < \Gamma_\infty \leqslant 190$ cm^2/s.

Let the radial and axial velocity components of the velocity field be expressed in terms of the dimensionless stream function $\bar{\psi}$ by

$$v_r = \frac{Q_s}{r_0 l \eta^{\frac{1}{2}}} \frac{\partial \bar{\psi}}{\partial \xi}, \tag{1}$$

$$v_z = \frac{-2Q_s}{r_0^2} \frac{\partial \bar{\psi}}{\partial \eta}, \tag{2}$$

and let the circumferential velocity component be expressed in terms of the dimensionless circulation $\bar{\Gamma}$ by

$$v_\theta = \frac{\Gamma_\infty \bar{\Gamma}}{2\pi r_0 \eta^{\frac{1}{2}}}, \tag{3}$$

where Γ_∞ is the circulation of the free vortex and Q_s is the volume rate of sink flow.

The dimensionless independent variables η and ξ are defined as

$$\eta = (r/r_0)^2, \tag{4}$$

$$\xi = z/l, \tag{5}$$

where r_0 is the radius of the sink orifice, and l is the water depth.

As shown by Granger (1972, 1973), the vortex produced in the cylinder closely approximated those vortex flows where the dimensionless circulation $\bar{\Gamma}$ is a linear function of the dimensionless stream function $\bar{\psi}$

$$\bar{\Gamma}/\bar{\psi} = Ro^{\frac{1}{2}}, \tag{6}$$

where Ro is the Rossby number

$$Ro = 2\pi Q_s / r_0 \Gamma_\infty. \tag{7}$$

The Rossby number can be viewed as a type of Froude number or as inversely proportional to the Squire parameter Sq. Much work on the theory of vortex breakdown in the past has been based on the Squire–Long equation (see Squire 1960). The view of Stuart (1987) is that vortex breakdown has a strong tendency towards stagnation on the axis occurring rather close to, but not exactly at some critical value of Sq. Similarly, there must be a low value of Ro that defines where disturbances may propagate along the axis (subcritical state) and a high value of Ro where no disturbances are possible (supercritical state).

Equation (6) easily leads to a relationship in which the ratio of the axial velocity to the vorticity about the axis of rotation is constant, a result borne out by the experimental measurements presented by Granger (1972).

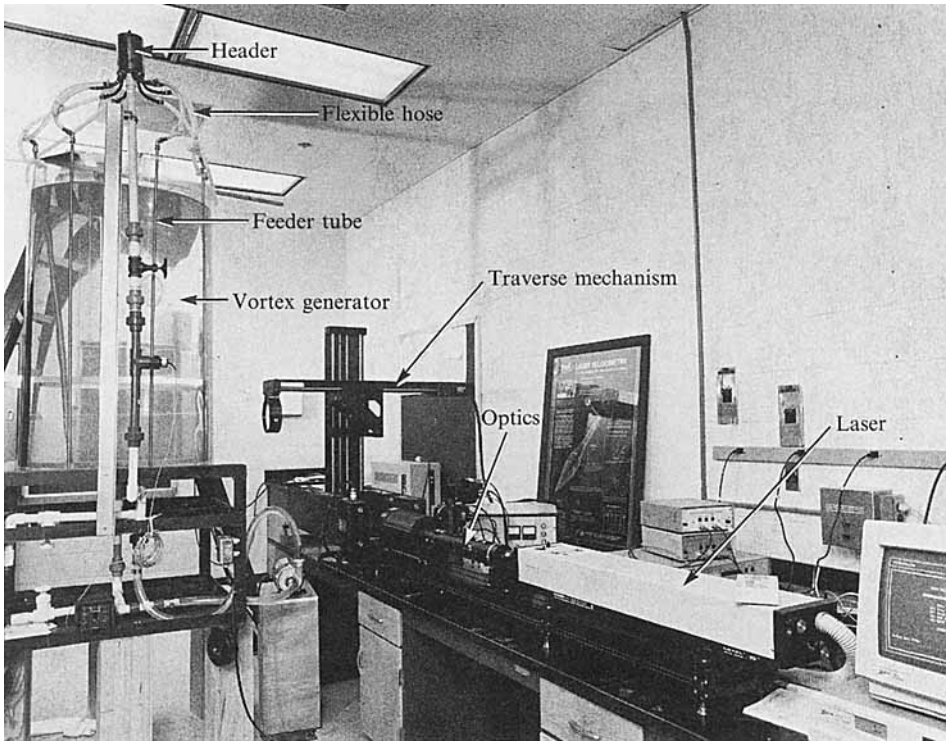

FIGURE 3. Layout of apparatus.

3. Measurement techniques

The radial and axial distributions of the tangential and axial velocity components were measured using a Thermal Systems Inc. (TSI) 9400 argon ion LDV that had a maximum beam power of 1.5 W compared to a rated 3.5 W power. The system incorporated three beams in the backscatter mode. Though this mode resulted in a lower data rate than a forwardscatter mode, it allowed for massive amounts of data to be collected with relative ease. The probe volume diameter based upon a 250 mm focal length was 117 μm and the fringe spacing was 2.67 μm. An automated traverse of the flow field in the central region of the tank was accomplished using a TSI mirror-mount traverse table. A photograph of the instrumentation setup is shown in figure 3.

The bottom and back of the vortex tank was painted flat black in order to reduce the signal-to-noise ratio in the boundary-layer measurements. This modification resulted in the data rate increasing nearly threefold. The data rate was also increased by seeding. The seed was silicon carbide no. 10081, having a 1.5×10^{-3} mm diameter. A slurry of 0.2585 g of silicon carbide in 1000 l of water was found to work best.

In order to visualize the flow, dichlorofluorescein mixed with water is fed into the centre of the vortex near the free surface. The slightly negative pressure at this point provided a natural mechanism by which the dye mixture could be injected without disturbing the flow. When the dye reached the sink, a sudden closing and opening of the sink spread the dye throughout the viscous core. Some of the dye re-entered the sink and was ingested back into the vortex through the hooded slots along the inner cylinder. Thus, the water in the inner cylinder was lightly mixed with the dye.

Spreading a laser beam of light with a glass rod produces sheet lighting. The sheet

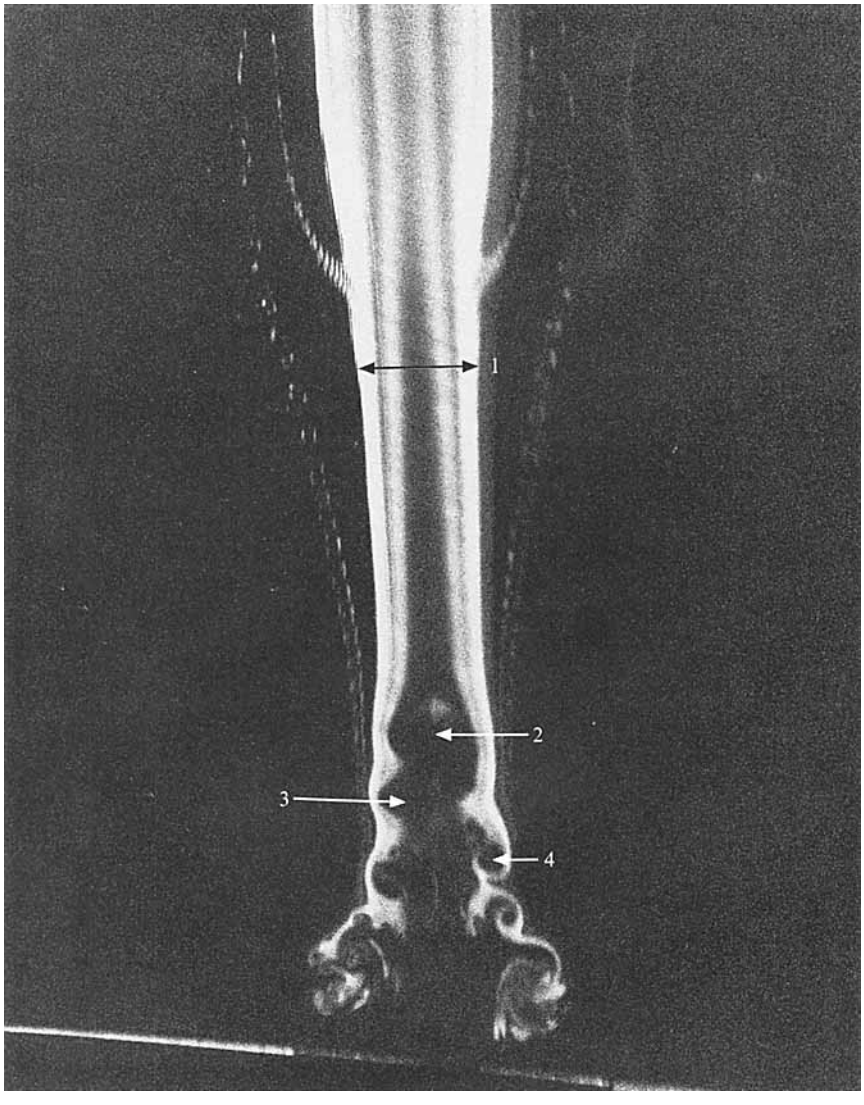

FIGURE 4. Laser sheet light visualizing the wake of the vortex breakdown: 1 is viscous core, r_c = 1.18 cm; 2 is front of vortex breakdown; 3 identifies one of two vortex spiral filaments; 4 vortex eddy. $\Gamma_\infty = 90$ cm^2/s, $r_0 = 0.635$ cm, $\xi = 0.924$, $\nu = 9.29 \times 10^{-3}$ cm^2/s.

lighting could be oriented in any desired plane by manipulating the rod. A video camera placed approximately 4 ft from the vortex cylinder was focused to take side-view pictures of the breakdown phenomenon illuminated by sheet lighting in an otherwise darkened environment.

4. The observations

As has already been stated, the search for secondary motion was based on exploring the structure of vortex breakdown. The circulation which proved most suitable for studying the breakdown was about 18 cm^2/s. The values of viscosity, sink-orifice radius, depth of water and other parameters were identical to those used by Granger (1972). Specific values of the parameters are given in the figure captions.

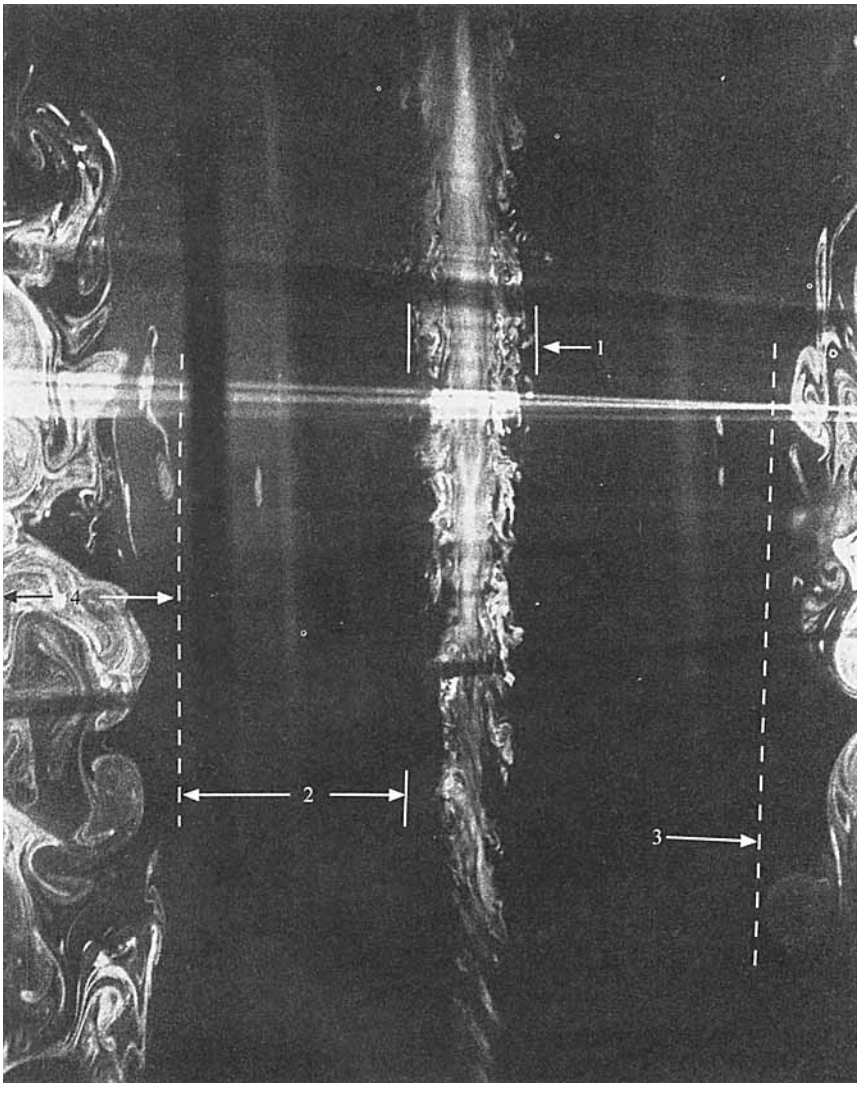

FIGURE 5. Side view of the vortex showing three distinct regions: 1 is the viscous core and turbulent wake region; 2 is the irrotational free-vortex region free of disturbances; 4 is the region of the turbulent shear layer. The inner edge of the turbulent shear layer is marked 3. $\Gamma_\infty = 90$ cm^2/s, $r_0 = 0.635$ cm, $\xi = 0.48$, $\nu = 9.29 \times 10^{-3}$ cm^2/s.

The procedure was simple. After an axisymmetric steady laminar vortex was established, the sink was momentarily closed, then opened so that a disturbance formed at the sink. Initially the disturbance was perfectly spherical (providing there were no disturbances in the vortex field), but then it degenerated into the spiral vortex of figure 4. The front of the disturbance is seen to be clearly within the viscous core, region 1. Vortex filaments are discernible and extend to three core diameters downstream in the wake. Most investigators might agree that transition such as that from laminar flow to vortex breakdown cannot occur without initial instability. The instability most often grows from zero amplitude to some maximum, the process being continuous. Also, investigators might agree that for a flow to be unstable, the

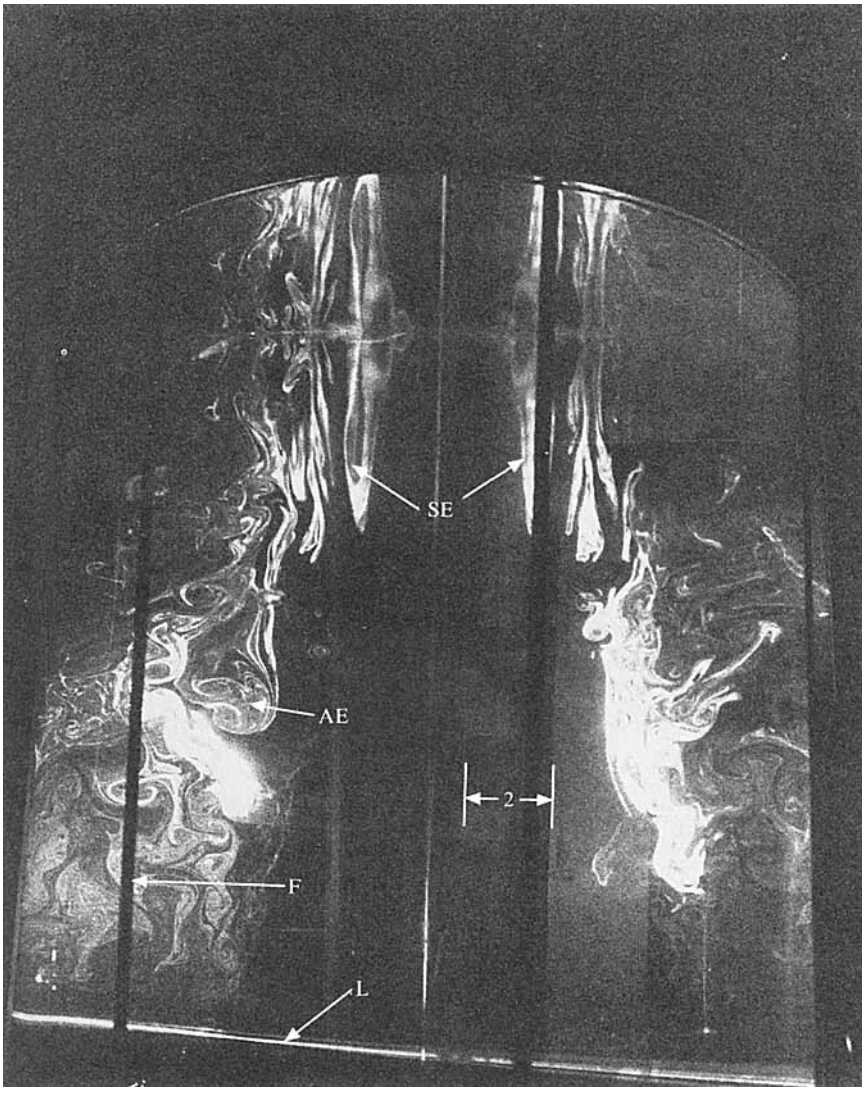

FIGURE 6. Side view of the upper half of the vortex visualized by laser sheet lighting. Note secondary motion near the free surface and complexity of vortical motion near mid-tank. SE denotes symmetric eddies, AE represents asymmetric eddies, F denotes feeder tube, L is the laser beam, and 2 is the inner region. $\Gamma_\infty = 90$ cm^2/s, $r_0 = 0.635$ cm, $\nu = 9.29 \times 10^{-3}$ cm^2/s.

disturbances must grow unchecked 'from little swirls to larger swirls and on to infinity'. It then seems reasonable that the field of instability degenerates into an unsteady motion. However, there are contradictions in this conjecture. Figure 1(*a*) shows transition. The instability occurred at the sink where the disturbance was formed. The disturbance is very stable and does not grow at all for the major length of its path. Also note that the wake is free of disturbance.

Figure 5, on the other hand, shows an unstable wake filled with disturbances in the viscous core, region 1. (In the discussion to follow all the photographs were taken using P3200 Kodak T-Max film at a shutter speed of $\frac{1}{30}$ s and an f-stop of 2.8; the light source was from the laser beam.) Downstream of the wake, the disturbances do

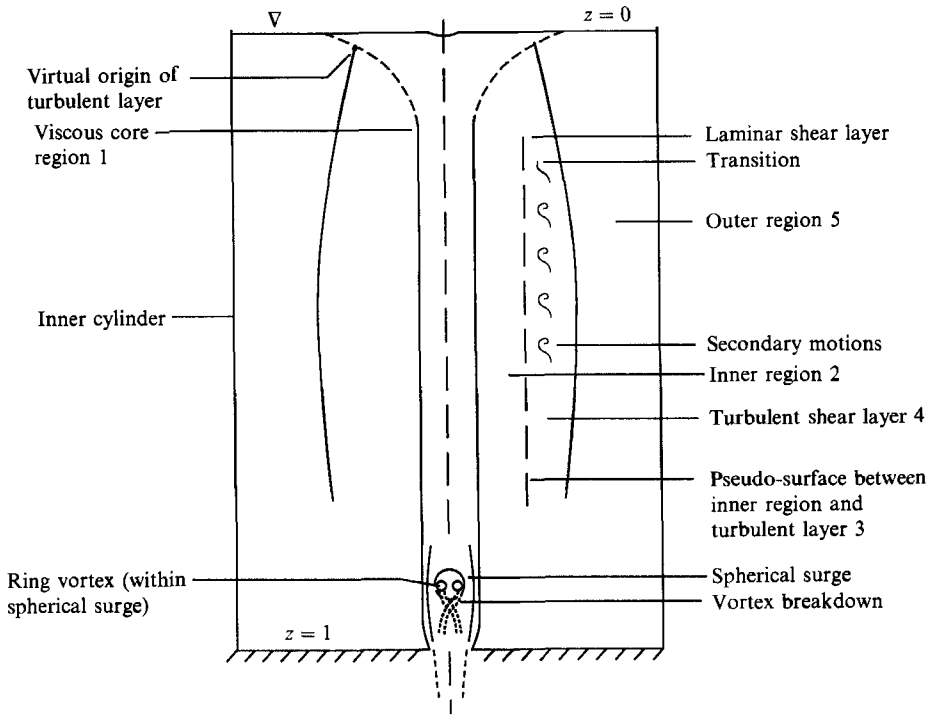

FIGURE 7. Schematic of the physical model of the vortex flow.

appear to die out, and the downstream flow appears to be reverting back to its former flow. This return to normal flow conditions, being nearly reversible, is an indication of criticality rather than instability. However, notice in region 4 of the figure that at a radius approximately 6 times the core radius, large-scale eddies have formed. These are what we are calling secondary motions.

These eddies have been detected earlier (see figure 9 of Escudier *et al.* 1982). They lie in an irrotational zone where no secondary motions had been measured (Granger 1972). This is the region in which the flow behaves as a free vortex, and we call this region the turbulent shear layer. The pseudo-boundary separating the inner region 2 from the turbulent shear layer is surface 3. Another view of these motions is presented in figure 6.

Figure 6 is a photograph of the upper half of the vortex apparatus. The dark upright lines are the feeder tubes, F. The bright lower and near-horizontal line is the laser beam. The photograph was taken after eleven disturbances had propagated along the centreline. The number of disturbances had little influence on the general pattern of the flow, provided that the flow in the core was allowed to settle back to steady-state conditions before another disturbance was created. In the photograph, the central dark region consists of the viscous core and an inner region. The inner region 2 is that annular volume between the viscous core and the turbulent shear layer. The inner region contains the multi-directional axial flow and the inner fringe of the turbulent shear layer. Within this zone, there is an annular radial region in which there is a reversal of direction in the circumferential velocity.† This reversal

† The reversal of direction in the circumferential velocity unfortunately cannot be observed by viewing still photographs. One may observe this phenomenon by borrowing VHS tape EMVC 902904, Vortex Breakdown, from ERC, US Naval Academy, Annapolis, MD 21402.

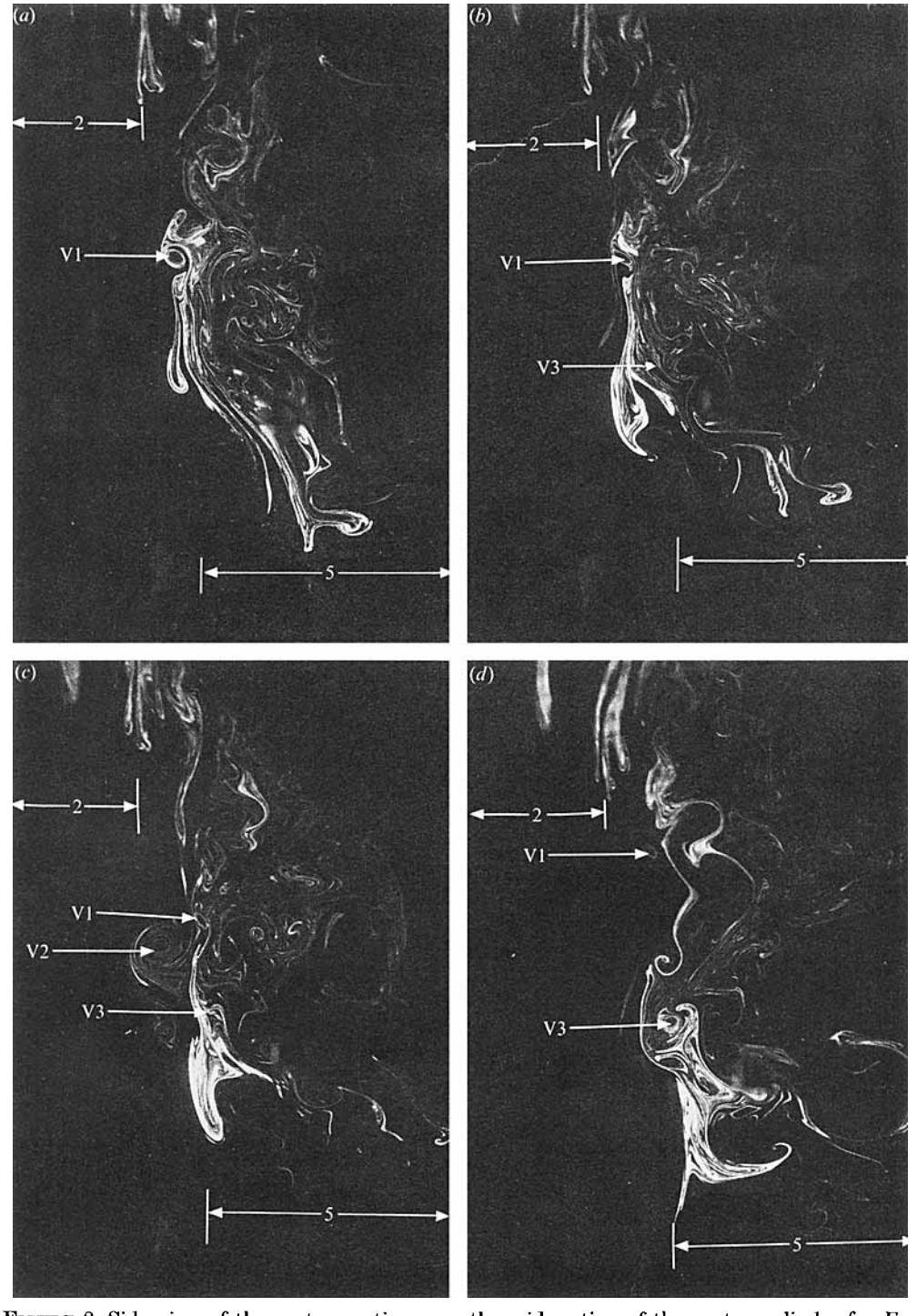

FIGURE 8. Side view of the vortex motion near the mid-section of the vortex cylinder for $\Gamma_\infty = 90\ \mathrm{cm^2/s}$, $r_0 = 0.635$ cm, $\xi = 0.3$, $\nu = 9.29 \times 10^{-3}\ \mathrm{cm^2/s}$. Axial flow is from the top to bottom and sense of rotation follows the right-hand rule; (*a*)–(*c*) are approximately 4 s apart, and (*d*) is 30 s after (*c*). For explanation of numerals see text.

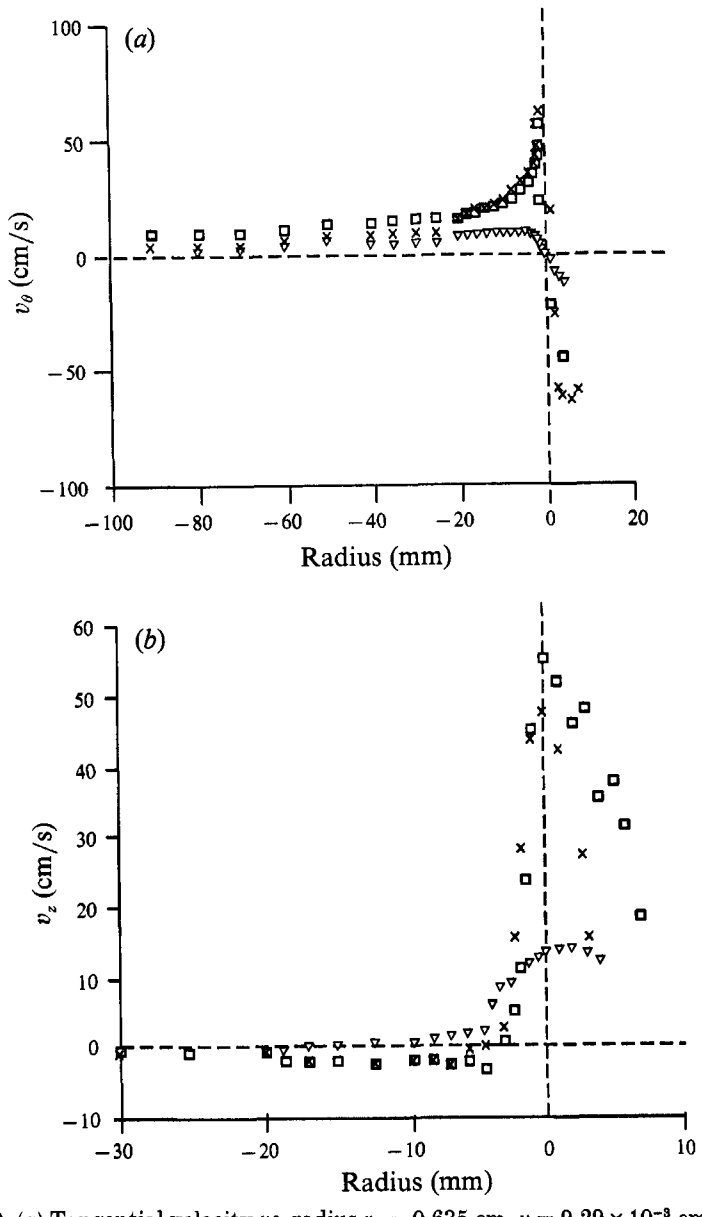

FIGURE 9. (*a*) Tangential velocity *vs.* radius $r_0 = 0.635$ cm, $\nu = 9.29 \times 10^{-3}$ cm^2/s. (*b*) Axial velocity *vs.* radius at a fixed depth for three flow rates: ▽, $\Gamma_\infty = 89$ cm^2/s; ×, 171 cm^2/s; □, 188 cm^2/s and $\xi = 0.95$, $r_0 = 0.635$ cm, $\nu = 9.29 \times 10^{-3}$ cm^2/s.

of direction is substantiated theoretically by Granger (1972) for steady laminar flow and for the case $\epsilon > 1.4$, where

$$\epsilon = zr^2/lr_c^2, \tag{8}$$

where r_c is the core radius and z is the vertical direction ($z = l$ at the sink). For unsteady laminar flow, a reversal of direction in circumferential velocity is also predicted theoretically by Granger (1973). It should be mentioned that the motions in these regions of vortex flow are independent of the orientation of the light sheet.

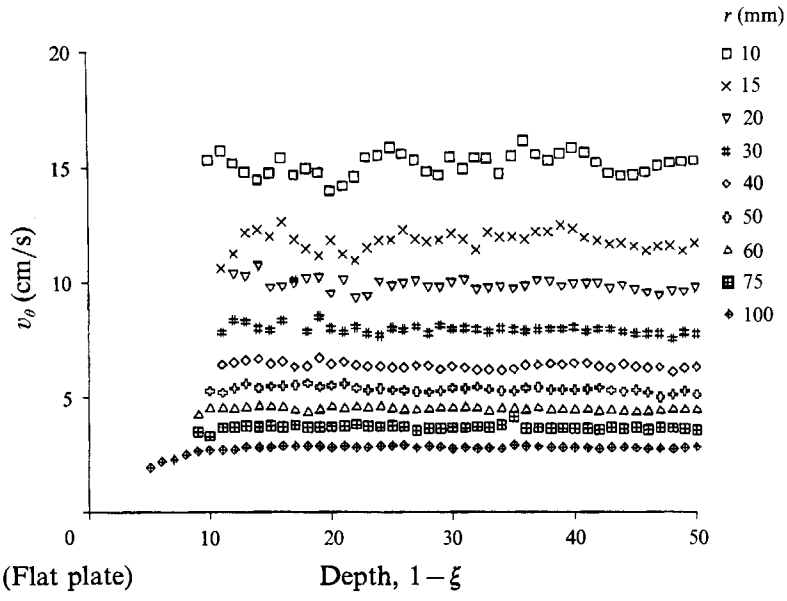

FIGURE 10. Tangential velocity outside the viscous core *vs.* depth. $\Gamma_\infty = 188$ cm^2/s, $r = 0.635$ cm, $\nu = 9.29 \times 10^{-3}$ cm^2/s, $r = 10$–100 mm.

A simplified schematic of the various regions is proposed in figure 7. An instantaneous picture of a vertical cut of the vortex (like that of figure 5) shows that the irrotational zone is dominated by a chain of large eddies, those near the free surface being symmetrical about the centreline (see SE in figure 6) and those at $z/l > 0.3$ being asymmetrical (AE in figure 6). The principal zones are 1, a rotational core of radius inversely proportional to the square root of the ambient circulation; 2, an inner region; 4, a turbulent shear layer within which large eddies form and whose diameters define the visual thickness of the shear layer; and 5, an outer region of smaller-scale eddies where secondary motions break up. This outer region is more clearly seen in figure 8.

The photographs of figure 8 show the visualization of the flow in a vertical plane at mid-depth. The axial flow is from the top to the bottom of each photograph, and the sense of rotation follows the right-hand rule. The sequence of photographs (*a*–*c*) were taken approximately 4 s apart whereas (*d*) was taken 30 s after (*c*). Note the vortical motions arising in the turbulent layer. The vortex denoted by V1 in the sequence of four photographs slowly dissolves with small rotational displacement and no appreciable axial displacement. Some vortices form, then disappear within 30 s as is illustrated by vortex V2, while others like V3 take almost a minute to form. The vortices are seen to break up in the outer region (the region 5 on the right-hand side of each photograph). No vortical or secondary motions exist in the inner region 2, as is evident from examining the vertical streakline fingers near the top of each photograph.

LDV profiles at various axial locations and for several flow rates confirm that the primary motion outside the viscous core is nearly irrotational. Figure 9(*a*) shows that the flow can be approximated by a simple Rankine vortex, and figure 9(*b*) reveals small to negligible axial velocities in the outer region. The two figures are but a sample of some of the extensive experimental data from LDV measurements which served to verify the earlier experimental measurements of Granger (1972). Thus,

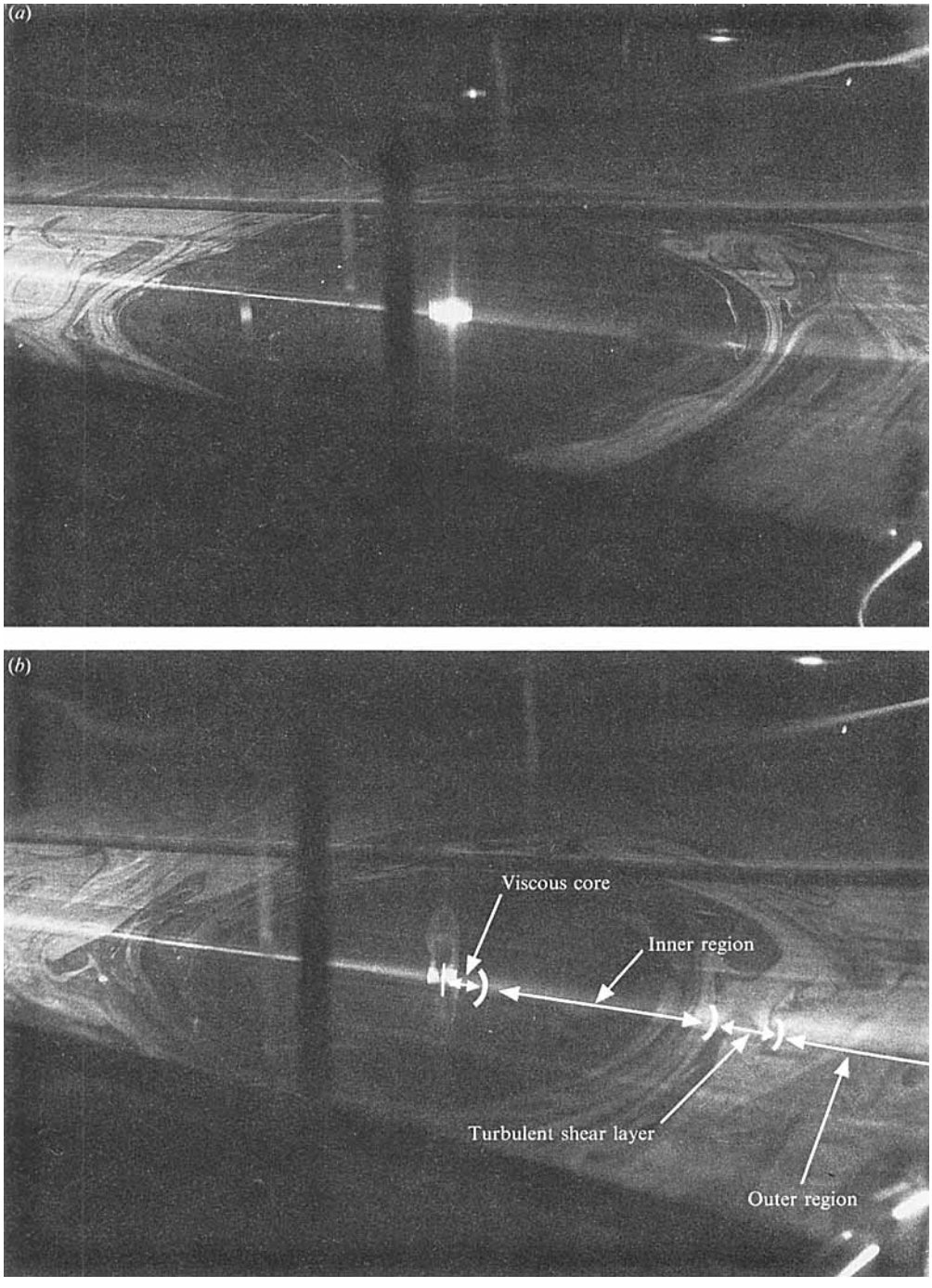

FIGURE 11 (*a*, *b*). For caption see facing page.

there is no need to present these measurements again. However, some comment should be made on estimating the accuracy of the velocity measurements. The Appendix presents a brief discussion of how the number of data points needed to obtain a good mean value for the velocity at a point in the flow field was determined.

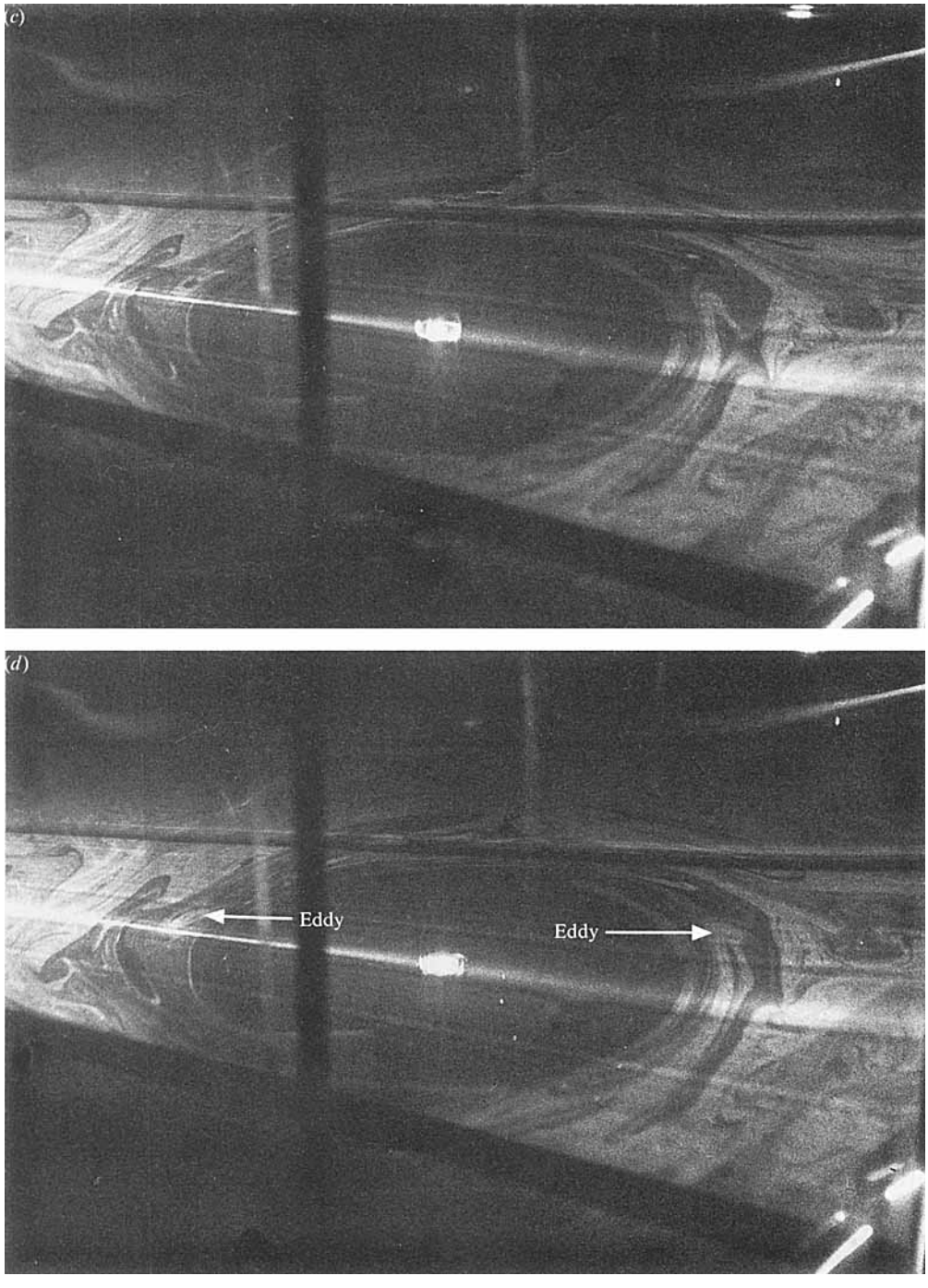

FIGURE 11. (*a*) Near top view of the vortex flow before breakdown, $\Gamma_\infty = 90$ cm^2/s, $r_0 = 0.635$ cm, $\xi = 0.5$, $\nu = 9.29 \times 10^{-3}$ cm^2/s. (*b*) Same position 9 s later than (*a*). (*c*) Same position 4 s later than (*b*). Note the radial confinement of the vortex wake. (*d*) Same position 4 s later than (*c*). Note no disturbances in the irrotational region.

Figure 10 shows LDV measurements of the axial distribution of the tangential velocity at nine radial locations for a fixed ambient circulation and sink orifice radius. If we take the data in figure 10 for $z/l = 0.95$ and plot the tangential velocity v_θ versus radius r, we will obtain the curve in figure 9(*a*) for $\Gamma_\infty = 188$ cm^2/s in the region outside the core. The data reveal that the velocity behaves as a Rankine vortex; but superimposed on the velocity is a secondary motion.

The secondary motion arises from an unsteady disturbance that propagated along the centreline with associated fluid motions that vary in time. As seen in figure 10, the motion is nearly sinusoidal and irregular at specific radii. We thus have the situation of waves that are within an otherwise completely steady irrotational flow. Although the axial variation may reveal a nearly sinusoidal variation, some of the motion exhibits little change with time (vortex V1 in figure 8) and others exhibit significant change with time (V3 in figure 8). Since the wave patterns were created by the spiral disturbance at the inner boundary of the flow, vortex breakdown is viewed as an instability phenomenon. If the disturbance in the turbulent shear layer could produce the vortex breakdown, it would be strong evidence attributing the phenomenon to instability. However, the data in figure 10 show that though the amplitude of the secondary wavelike motion does grow as the vortex centreline is approached, the secondary motion does *not* extend into the inner region (region 2 in figure 8). This characteristic is attributed to how the flow is fed into the core. Granger (1972) showed in a typical cross-section of the stream tubes that the fluid motion is from the boundary layer at the plate up towards the free surface and outwards into the inner region, then inwards towards the centreline and out through the sink. Any disturbances that are formed in the region outside the viscous core decay in the feeding of the flow into the viscous core. Thus, if no disturbances are present in the vortex (regions 1–5) when the disturbance is formed at the sink, the flow in the core will close around the disturbance, encapsulating the disturbance in the form of a sphere and resulting in the disturbance propagating along the centreline towards the free surface with kinematics described by Granger (1968). However, if *any* disturbance exists in any of the regions of the vortex field, even the outer region 5, then disturbance formed at the sink will quickly break down into a vortex spiral filament like that shown in figure 1(*c*).

When we explore this phenomenon in greater detail, flow visualization reveals the existence of a highly disorganized secondary motion. The interaction of ring vortices, jets and eddies with the large-scale eddies in the turbulent shear layer produces a conglomeration of assorted secondary motions involving slip-through of pairs of vortex rings, vortex feeding and decay, and jet plumes forming ring vortices, the latter noted near the middle of figure 8(*a*).

Turning a glass rod rotates the sheet of laser light from the vertical plane to a horizontal plane. Figure 11 is a sequence of photographs showing a plane of laser light at mid-depth and inclined at approximately 10° from the horizontal. Photograph (*b*) was taken 9 s after (*a*) whereas the other three photos were taken 4 s apart. All other parameters such as circulation were fixed. The central spot of light in each photo represents the cross-section of the viscous core. Figure 11(*a*) is before vortex breakdown has reached the point of intersection formed by the laser sheet of light and the vortex centreline. Figure 11(*b*) shows the vortex breakdown with its two vortex filaments propagating towards the free surface. The filaments are rotating counter to the sense of the mean flow. This lends support to the instability explanation for vortex breakdown. Vortex flows have been found to be unstable only for the case of counter-rotating helical disturbance (see Escudier & Zehnder 1982)

though, as pointed out by Escudier (1988), there is no reason for the origin of the disturbances always to be of the same rotating nature. Figure 11(*c*) shows the vortical wake 4 s later. Figure 11(*d*) shows the streakline pattern 8 s after the disturbance moved past the mid-depth position. Note that the inner region is relatively undisturbed by the breakdown. There are no visible wave patterns in the region nor were any detected (see figure 10). The barely discernible spiral pathlines in figure 11(*c*, *d*) are in the region representing the critical diameter wherein eddies formed by the vortex breakdown are confined (compare figure 11 with figure 4). Transition occurs near the outer edge of the inner region though two eddies are seen in figure 11(*d*) to be close to the radial region of transition. Videotapes revealed that the reversal of direction in the circumferential velocity of the primary flow in a small radial region of this turbulent shear layer region discussed earlier is as predicted by theory (Granger 1972). Moving outside the turbulent shear layer, one again notes the unusual dye patterns formed by interaction of the eddies and their decay.

At this point, two striking observations can be drawn from the results. For both low and high ambient circulations, the classical viscous core and irrotational vortex were obtained with eddies and secondary motion in the vortex field. There were also reversals of flow directions in both the axial and circumferential directions, resulting in what is classically called a multicell vortex structure. The primary flow behaves exactly as reported earlier by Granger (1972).

The second observation is that after a disturbance is formed and propagates along the centreline, the instabilities in the wake die out in the viscous core but not in the turbulent shear layer. This finding would appear to help support the contention that vortex breakdown is an instability phenomenon, at least for this type of confined vortex flow. This finding does not refute the opinion that the breakdown consists of two conjugate states, nor does it refute the claim that it is a stagnation phenomenon since stagnation still plays a key role in the behaviour of the disturbance. Breakdown is certainly a transition between a well-defined laminar flow upstream of the disturbance and a turbulent wake downstream of the disturbance. But examination of the vortex motion, especially in the far field, points to the breakdown being triggered by an instability and that that instability (in regions 4 and 5) persists for a considerable period. The vorticity is transported out to the shear layer, with large eddies being created from the shear that results from the reversed axial flow near the viscous core and an axial flow of smaller magnitude outside the core. With accompanying circulation superimposed on the shear, large-scale vortices form that are embedded in the turbulent shear layer. Those vortices interact with other eddies formed by previous disturbances.

At this stage in the experimentation, the first of these observations could be affirmed with certainty, but not so the second. At no time was it noticed that the flow outside the turbulent shear layer returned to its original undisturbed state, yet inside the viscous core the disturbed state always returned to its undisturbed state sometimes almost immediately provided that no disturbances were introduced or reflected at the free surface. Thus, the process was reversible in one region and not the other.

5. A résumé of the findings

(i) The breakdown can be a solitary spherical disturbance with laminar flow upstream and downstream, or a bubble-like disturbance, or a spiral-type disturbance with a turbulent wake consisting of at least two helical vortex filaments.

(ii) The vortex breakdown is confined approximately to the core and its size is inversely proportional to $\Gamma_\infty^{\frac{1}{2}}$.

(iii) Vortex breakdown is observed to be largely an instability problem since the flow degenerates into an unsteady motion in the turbulent shear layer where the initial perturbation grows unchecked.

(iv) Observations are made on a vortex whose dimensionless circulation is proportional to the dimensionless stream function, the constant of proportionality being the square root of the Rossby number.

(v) New regions of secondary motions are identified in the irrotational region of an otherwise steady vortex flow, motions that have as yet no theoretical basis.

Owing to the elusive nature of the secondary motions in the irrotational region, more decisive testing is very difficult. Thus, conclusion (v) is at best poorly defined. In fact, it is not truly a finding but a prescribed property of the flow field. Conclusion (iv) is substantiated by Granger's theoretical analysis (1972, 1973). The merits of this experiment have been in helping to identify the breakdown as principally an instability problem rather than one of critical states; and in demonstrating that a turbulent shear layer exists in internal vortex sink flows with large-scale asymmetric vortices and higher-order secondary motions in a field far removed from the core even though a normal vortex had been restored in the core.

I am indebted to D. Reckamp for his contributions in the experimental measurements, to Drs H. Lugt (NSRDC) and O. M. Phillips (JHU) for their lively interest.

Appendix. Accuracy of the velocity measurements

In this appendix, we address the question of how many data points were used to obtain a good mean value and/or standard deviation. A reasonable value was obtained based on the work of Donohue, McLaughlin & Tiederman (1972) and Yanta & Smith (1973). Let X be the sample mean, μ the population mean and σ the population standard deviation. The confidence limits for estimating the population mean are given by

$$\mu \leqslant X \pm z_c \sigma / N^{\frac{1}{2}}, \tag{A 1}$$

where z_c equals 1.645, 1.96 and 2.58 for 90, 95 and 99% confidence limits, respectively. Since σ is unknown, we use the sample standard deviation σ_s which is allowed if $N \gg 100$. Assuming N is sufficiently large such that $(N-1)^{\frac{1}{2}} \approx N^{\frac{1}{2}}$ and $z_c \approx 2.0$ for a 95% confidence limit, then the number of data points

$$N = 4(\sigma/\mu)^2/(\mu - X/\mu)^2 \tag{A 2}$$

and the population standard deviation is

$$\sigma \leqslant \sigma_s \pm 2\sigma/N^{\frac{1}{2}}.$$

The error in the standard deviation equals $2/2N^{\frac{1}{2}}$, or the number of data points equals $2/(\text{error})^2$. Hence the number of data points needed for the standard deviation is independent of the flow conditions. For the present test, a 95% confidence level was assumed. This meant that a minimum of approximately 800 data points was needed to ensure that the sample deviation did not differ by more than 5% from the true population standard deviation.

REFERENCES

BENJAMIN, T. B. 1962 Theory of the vortex breakdown phenomenon. *J. Fluid Mech.* **14**, 593.

BOSSEL, H. H. 1969 Vortex breakdown flow field. *Phys. Fluids* **12**, 498.

CASSIDY, J. J. & FALVEY, H. T. 1970 Observations of unsteady flow arising after vortex breakdown. *J. Fluid Mech.* **41**, 727.

CHANAUD, R. C. 1965 Observations of oscillatory motion in certain swirling flows. *J. Fluid Mech.* **21**, 111.

CHURCH, C. R., SNOW, J. T. & AGEE, E. E. 1977 Tornado vortex simulation at Purdue University. *Bull. Am. Met. Soc.* **58**, 900.

DONOHUE, G. L., MCLAUGHLIN, D. K. & TIEDERMAN, W. G. 1972 Turbulence measurements with a laser anemometer measuring individual realizations. *Rep.* ER 72-F-11. School of Mech. & Aero. Engng, OK State University.

ESCUDIER, M. P. 1984 Observations of the flow produced in a cylindrical container by a rotating endwall. *Exps Fluids* **2**, 189.

ESCUDIER, M. P. 1989 Vortex breakdown: observation and explanations. *Prog. Aerospace Sci.* **25**, 189.

ESCUDIER, M. P., BORSTEIN, J. & MAXWORTHY, T. 1982 The dynamics of confined vortices. *Proc. R. Soc. Lond.* A **382**, 355.

ESCUDIER, M. P., BORSTEIN, J. & ZEHNDER, N. 1980 Observations and LDA measurements of confined turbulent vortex flow. *J. Fluid Mech.* **98**, 49.

ESCUDIER, M. P. & ZEHNDER, N. 1982 Vortex flow regimes. *J. Fluid Mech.* **115**, 105.

FALER, J. H. & LEIBOVICH, S. 1977 Disrupted states of vortex flow and vortex breakdown. *Phys. Fluids* **20**, 1385.

GARG, A. K. & LEIBOVICH, S. 1979 Spectral characteristics of vortex breakdown flowfields. *Phys. Fluids* **22**, 2053.

GRANGER, R. A. 1966 Steady three-dimensional vortex flow. *J. Fluid Mech.* **25**, 557.

GRANGER, R. A. 1968 Speed of a surge in a bathtub vortex. *J. Fluid Mech.* **34**, 651.

GRANGER, R. A. 1972 A steady axisymmetric vortex field. *Geophys. Fluid Dyn.* **3**, 45.

GRANGER, R. A. 1973 On the decay of a viscous vortex. *Q. Appl. Maths* **30**, 531.

HALL, M. G. 1972 Vortex breakdown. *Ann. Rev. Fluid Mech.* **4**, 195.

KINNEY, R. B. 1967 Universal velocity similarity in fully turbulent rotating flows. *Trans. ASME* E: *J. Appl. Mech.* **34**, 437.

LAMBOURNE, N. C. & BRYER, D. W. 1962 The bursting of leading-edge vortices – some observations and discussion of the phenomenon. *UK Aero. Res. Counc. R & M* 3282.

LEIBOVICH, S. 1978 The structure of vortex breakdown. *Ann. Rev. Fluid Mech.* **10**, 221.

LEIBOVICH, S. 1983 Vortex stability and breakdown: Survey and extension. *AIAA J.* **22**, 1192.

LUDWEIG, H. 1961 Erganzung zu der Arbeit: 'Stabilitat der Stromung in einem zylindrischen Ringraum'. *Z. Flugwiss* **9**, 359.

LUDWEIG, H. 1964 Experimental verification of the stability theory for inviscid flows with helical streamlines. *Z. Flugwiss* **12**, 304.

LUGT, H. 1962 Ein der Drallstromung auf die Durchflusszahlen genormeter Drosselmessgerate. *Rep. Br. Hydromech. Res. Ass.* T716.

LUGT, H. & ABBOUD, M. 1987 Axisymmetric vortex breakdown with and without temperature effects in a container with a rotating lid. *J. Fluid Mech.* **179**, 179.

MAXWORTHY, T. 1974 Turbulent vortex rings. *J. Fluid Mech.* **64**, 227.

MAXWORTHY, T. 1977 Some experimental studies of vortex rings. *J. Fluid Mech.* **81**, 465.

MORGAN, G. 1951 A study of motions in a rotating liquid. *Proc. R. Soc. Lond.* A **206**, 108.

MURTHY, S. N. B. 1971 Survey of some aspects of swirling flows. *Aero. Res. Lab. Rep.* ARL 71-0244, p. 299.

OSER, H. 1957 Erzwungene Schwingungen in rotierenden Flussigkeiten. *Arch. Rat. Mech. Anal.* **1**, 81.

ROTT, N. & LEWELLEN, W. 1966 Boundary layers and their interactions in rotating flows. *Prog. Aerospace Sci.* **7**, 111.

SARPKAYA, T. 1971 On stationary and travelling vortex breakdown. *J. Fluid Mech.* **45**, 545.

SQUIRE, H. B. 1960 Analysis of the 'vortex breakdown' phenomenon. Part I. *Imperial College Aero. Dept. Rep.* 102.

STUART, J. T. 1987 A critical review of vortex-breakdown theory. In *2nd Intl Colloq. in Vortical Flow, Baden, Switzerland*. BBC SFB 25.

THOMSON, SIR WILLIAM 1910 Vibrations of a columnar vortex. In *Mathematical and Physical Papers*, p. 162. Cambridge University Press.

WEDEMEYER, E. 1982 Vortex breakdown. *AGARD-VKI Lecture Series* 121.

WESKE, J. & RANKINE, T. 1963 Generation of secondary motions in the field of a vortex. *Phys. Fluids* **6**, 1397.

WIDNALL, S. 1975 The structure and dynamics of vortex filaments. *Ann. Rev. Fluid Mech.* **7**, 141.

YANTA, W. J. & SMITH, R. A. 1973 Measurements of turbulence-transport properties with a laser Doppler velocimeter. *AIAA Paper* 73-169.